STRONGLY HOM-DAMPED MULTI-CELL RF CAVITIES FOR HIGH-CURRENT APPLICATIONS*

R. Rimmer*, H. Wang, G. Wu, JLAB, Newport News, VA, USA

Abstract

Strongly HOM-damped single-cell cavities have been used for some time in storage rings where modest voltage and high beam current are required. Future high-current applications such as electron cooling or high-powered free electron lasers based on energy-recovered linacs would benefit from similarly damped multi-cell structures. We explore the possibilities for applying strong HOM damping techniques to multi-cell structures. We use modern simulation techniques to compare several commonly used methods such as beam-pipe damping, coaxial and waveguide dampers, and the influence of number of cells and cell shape on the resulting impedance. ("Superstructures" consisting of more than one multi-cell cavity are not covered here but are discussed elsewhere at this meeting). We also consider the possibilities for even stronger damping, if required, and discuss the implications for cavity construction and performance that might result from these changes.

INTRODUCTION

Strong HOM damping in accelerator RF cavities has become increasingly important as average current and machine performance push ever higher. Storage rings for light sources and colliders now routinely operate with strongly HOM damped single-cell cavities at Ampere current levels [1,2]. Linear colliders are proposed that rely upon moderate HOM damping of large numbers of multi-cell cavities to combat beam break up (BBU). Next generation machines based on energy recovering linacs (ERL's), including light sources and electron coolers, require a combination of high-gradient multi-cell structures and strong HOM damping. Some designs of HOM damped few-cell structures have already been used with success at moderate currents, e.g. in HERA [3]. We attempt to study some of the factors that influence the ultimate performance of multi-cell coupled-cavity structures by use of numerical simulations

SIMULATION METHOD

We used the time domain module in MAFIA with a simulated bunch to excite the cavity either on or off axis [4]. By recording the wake potential behind the bunch and taking a Fourier transform we were able to calculate the broad-band impedance spectrum. We used the waveguide boundary condition to terminate the beam pipes and any damping apertures attached to the structure. We have not attempted to model the small coaxial DESY type couplers with this method due to the high mesh density needed.

* This manuscript has been authored by SURA, Inc. under Contract No. DE-AC05-84ER-40150 with the U.S. Department of Energy.

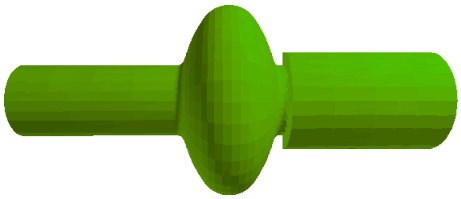

Figure 1a: Single enlarged beam pipe.

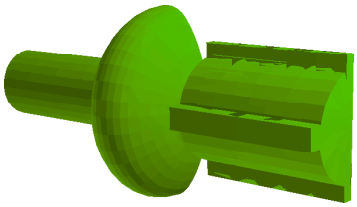

Figure 1b: Fluted beam pipe.

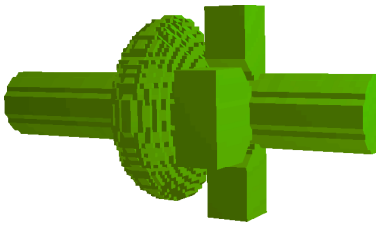

Figure 1c: Waveguide dampers.

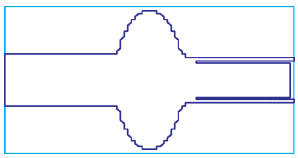

Figure 1d: Coaxial beam pipe.

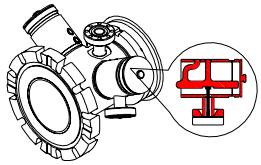

Figure 1e: Multiple coaxial loops.

BROAD-BAND DAMPING METHODS

Various schemes have been used to provide strong HOM damping on single-cell cavities and some have already been used on multi-cell cavities. The simplest method of HOM damping is to enlarge the beam pipe on one or both sides of the cavity so all harmful HOMs may propagate away, fig. 1a. This method has been used at KEK on the B-factory SCRF cavity [5]. A modification of this is the fluted beam pipe fig. 1b, used by Cornell on the CESR-B cavity [6]. This selectively lowers the cut-off frequency of the pipe for TE modes compared to the monopole TM modes allowing for a more compact structure. Waveguide dampers in the beam pipe just outside the cavity, fig. 1c, have been used in CEBAF [7], and potentially offer a way to remove large amounts of HOM power with very little increase in the axial length of the cavity. A coaxial insert in the beam pipe can also be

used to extract HOM power, fig. 1d, and this has been proposed for low-order mode damping in deflecting "crab" cavities [8]. It may be a way to make a compact beam-pipe load that separates the HOM-absorbing material from the beam. A choke may be used to reject the fundamental mode power. Coaxial HOM couplers fig. 1e, with built in notch filters to reject the fundamental mode are also widely used and can give strong coupling if placed appropriately. Normal conducting cavities may use openings directly into the accelerating cells for strong HOM damping. Conventional wisdom dictates that this may not be used for SCRF cavities, though it may be worth reconsidering in some circumstances, such as applications with modest gradient needs but high current.

We compared the beam pipe, waveguide and beam-pipe- coaxial damping methods using a MAFIA model of a single-cell 1.5 GHz cavity. Figure 2 shows the calculated response and table 1 shows the resulting loaded Q's and impedance for the strongest monopole HOM (TM_{011}). Clearly the beam-pipe damping on one or both sides (a,e) or with flutes (b) is very effective. The waveguide dampers (c) also give very good damping and the coaxial load (d) is not far behind. (This might be further improved by optimizing the geometry).

Figure 3 and table 2 show the results for the first two dipole HOMs (TE_{111}, TM_{110}). The impedance is calculated with the beam offset 25mm in the cavity. Strong damping is also evident in all cases, although there is more difference between the beam-pipe and waveguide methods in this instance.

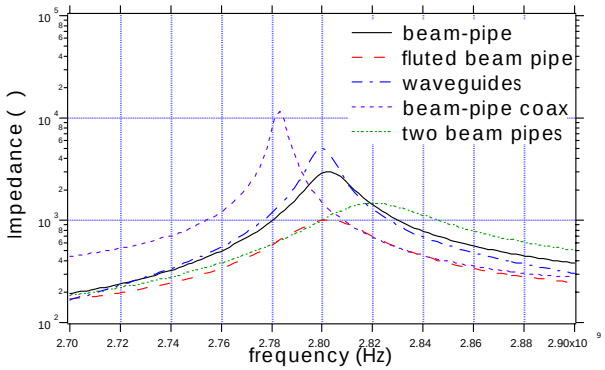

Figure 2: TM_{011} mode with various damping schemes.

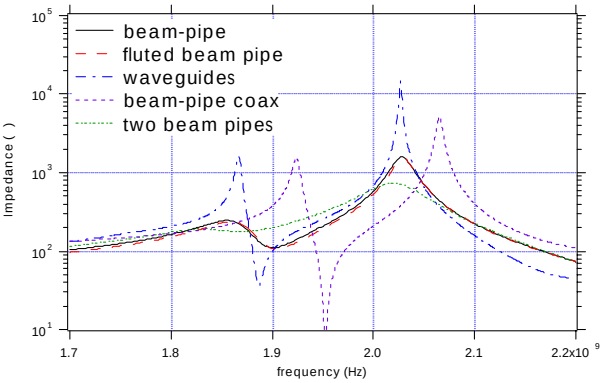

Figure 3: TE_{111}/TM_{110} modes with various dampers.

Table 1: TM_{011} mode for various damping methods

	freq MHz	Q_{ext}	R* (Ω)	R/Q (Ω)
a) b-pipe	2803	252	3001	11.9
b) flutes	2803	137	1010	7.3
c) w-guide	2800	353	5040	14.3
d) bp-coax	2783	725	11879	16.4
e) 2xbp	2822	121	1481	12.2

*$R=V^2/2P$

Table 2: Dipole modes for various damping methods

	TE_{111} f,MHz	TE_{111} Q_{ext}	TE_{111} R*, (Ω)	TM_{110} f, MHz	TM_{110} Q_{ext}	TM_{110} R* (Ω)
b-pipe	1853	83	246	2028	130	1567
flutes	1857	79	239	2029	130	1479
w-guide	1867	553	1594	2027	1131	14419
coax	1924	341	1496	2065	502	5150
2xbp	1830	37	192	2018	53	735

*R calculated at 25mm offset in the cavity

MULTI-CELL STRUCTURES

Given the strong results of each method on single cells we looked at the factors that may limit HOM damping performance of multi-cell structures.

Number of Cells

To study the dependence of damping on the number of cells we took one cell shape, with open beam pipes on both ends, and calculated the monopole and dipole spectra with from one to seven cells per cavity. Figures 4 and 5 show the calculated response for the TM_{011} and TE_{111}/TM_{110} passbands respectively. Tables 3 and 4 list the mode parameters for the strongest peak in each passband. Figures 6 and 7 show how the Q and impedance vary with number of cells. The strength of the highest mode in each passband increases with number of cells slightly faster than linearly. The Q's are also rising as the structures get longer, more or less monotonically for the TM_{011} and TE_{111} modes. Interestingly the TM_{110} mode seems to show a bifurcation with even numbers of cells having consistently higher Q's than odd numbers. The resulting impedance however climbs monotonically.

These results suggest that shorter structures might give better overall HOM performance than long ones, but at least in this range, the overhead in length from each HOM load or set of loads may mean the improvement is accompanied by a decrease in real estate gradient. This loss might be offset by sharing HOM loads and power couplers between adjacent cavities in "superstructure" assemblies [9]. In practice the maximum number of cells at a given frequency may also be dictated by physical infrastructure constraints, or limits on beam loading, window power or HOM load dissipation.

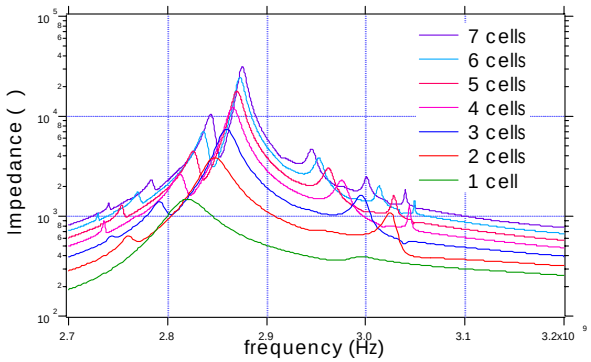

Figure 4: TM_{011} passband mode vs # cells.

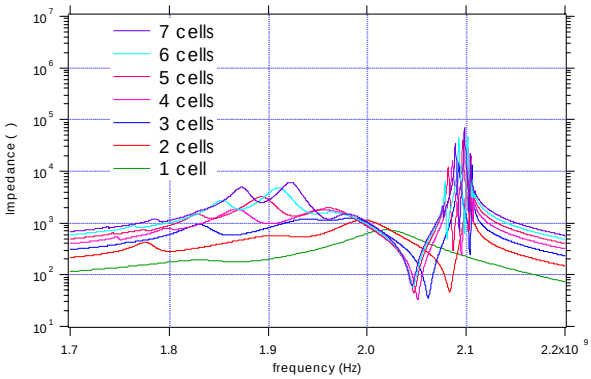

Figure 5: TE_{111} and TM_{110} passbands.

Table 3. TM_{011} monopole passband vs # cells

#cells	freq MHz	Q_{ext}	R* (Ω)	R/Q (Ω)
1	2822	121	1481	12.2
2	2848	167	3856	23.0
3	2860	219	7369	33.7
4	2866	295	12140	41.1
5	2870	362	17795	49.1
6	2873	455	24360	53.5
7	2876	527	31463	59.7

*$R=V^2/2P$

Table 4: Dipole passbands vs # cells

#cells	TE_{111} freq MHz	TE_{111} Q_{ext}	TE_{111} R* (Ω @25mm)	TM_{110} freq MHz	TM_{110} Q_{ext}	TM_{110} R* (Ω @25mm)
1	1830	37	192	2018	53	735
2	1907	46	569	2101	2641	10103
3	1940	45	1193	2093	2023	14362
4	1867	94	1844	2101	4058	29270
5	1892	121	3232	2097	3233	40923
6	1910	139	4859	2102	5029	46740
7	1922	135	6088	2099	4177	72101

*R calculated at 25mm offset in the cavity

Cell Shape, Cell- to-Cell Coupling

In order to look at the effect of cell shape and coupling strength between cells we compared seven-cell cavities with three different cell types, the original Cornell (OC), high-gradient (HG) and low-loss (LL) types. These shapes have different profiles, iris diameters and cell-to-cell coupling [10]. The OC shape has the highest coupling while the LL has the lowest. Figures 8 and 9 show the monopole and dipole spectra, while tables 5 and 6 list the peak values for the three passbands. The TM_{011} mode response is similar for the OC and HG shapes, while the LL peak is lower in frequency but similar in amplitude (within about a factor of three).

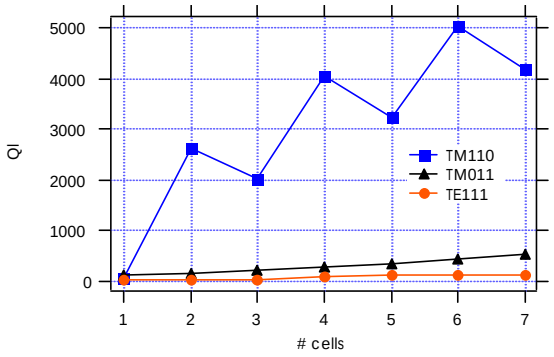

Figure 6: Loaded Q vs # cells, beam-pipe damping.

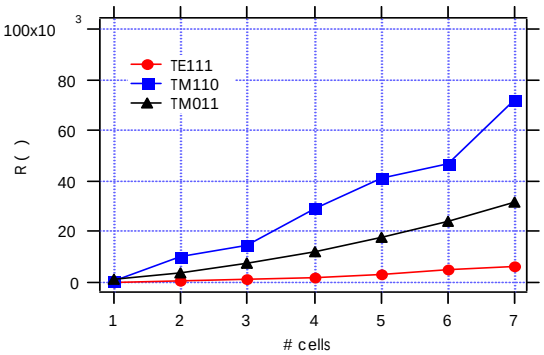

Figure 7: R vs # cells (R at 25mm for dipole modes).

The dipole passbands show different frequency response for all three cell types and about a factor of two spread in amplitude for the TE_{111} mode and about a factor of four in the TM_{110} mode. There does not appear to be any correlation between mode strength and cell-to-cell coupling in this data. For a given bunch spacing the exact frequency spectrum could make a significant difference in BBU threshold and HOM power between different cell shapes, so cell profile may be important in this regard.

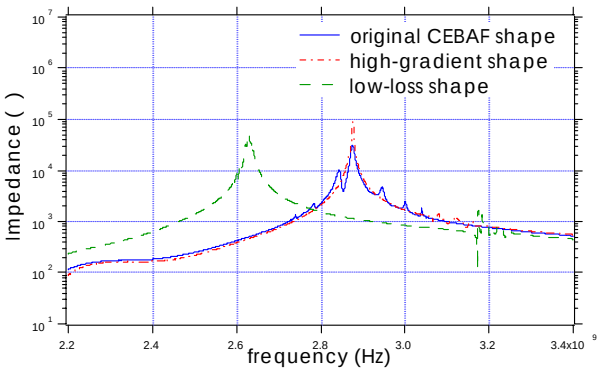

Figure 8: TM_{011} band, OC, HG, LL shapes, 7-cells.

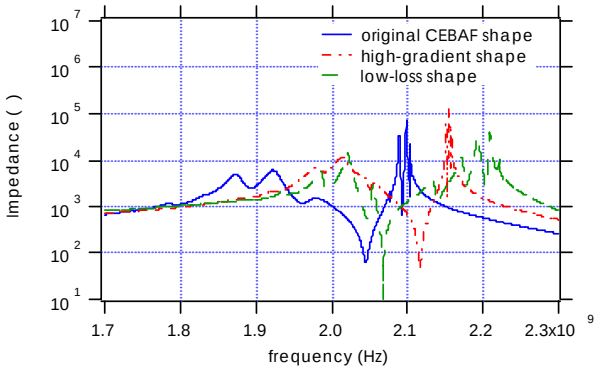

Figure 9: 7-cells, OC, HG, LL shapes, TE_{111}/TM_{110} dipole.

Table 5: TM_{011} mode data for multi-cell cavities.

	#cells	Freq,MHz	Q_{ext}	$R^{\dagger}$ (Ω)	R/Q (Ω)
OC	7	2876	527	31463	59.7
HG	7	2876	1348	90380	67.0
LL	7	2629	985	53556	54.4
OC*	5	2871	707	35453	50.1
DESY	4	910	600		

*waveguide damped. **500 MHz cavity, meas. Q. $^{\dagger}R=V^2/2P$

Table 6: TE_{111}/TM_{110} mode data for multi-cell cavities.

	# cells	TE_{111} f,MHz	TE_{111} Q_{ext}	TE_{111} $R^{\dagger}$, (Ω)	TM_{110} f, MHz	TM_{110} Q_{ext}	TM_{110} $R^{\dagger}$ (Ω)
OC	7	1922	135	6088	2099	4177	72101
HG	7	2014	185	11359	2156	5694	146409
LL	7	2021	490	14107	2209	2071	39510
OC*	5	1894	956	22949	2103	3274	47064
DESY	4	650	4000		716	6000	

*waveguide damped. †R calculated at 25mm offset in cavity.

EXAMPLES

Figure 10 shows a five-cell structure with waveguide damping. The highest peaks in each passband are listed in tables 5 & 6 (row 4). The TM_{011} peak is about a factor of two stronger for the waveguide damped cavity than for the beam pipe loaded one (Fig. 11), (table 3 row 5). For the TE_{111} mode (table 4 row 5), the factor is about eight but for the strongest dipole (TM_{110}) mode they are about the same, Fig. 13. The waveguide dampers take up very little beam line space compared to the beam pipe loads and can transport HOM power to room temperature loads if required. These factors may be important in a large machine where the length of the accelerator section and/or cryogenic heat load are constrained.

Included in tables 5 & 6 are data for a four cell 500 MHz DESY cavity damped by three coaxial HOM couplers [3]. The TM_{011} Q_{ext} is very similar to the waveguide loaded cavity while the TE_{111} Q_{ext} is a factor of four higher and the TM_{110} is only up about a factor of two.

All of these examples are in the range suitable for next generation high current machines.

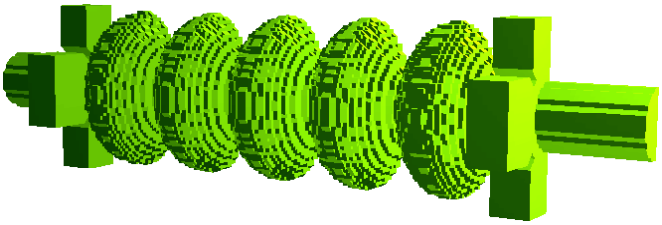
Figure 10: Waveguide damped 5-cell structure.

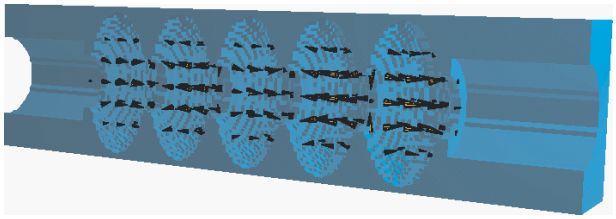
Figure 11: Beam pipe damped 5-cell structure.

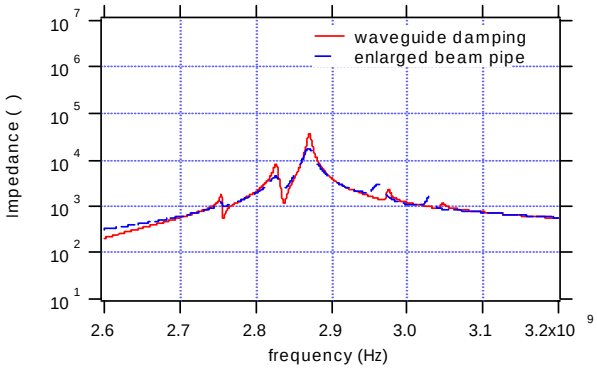

Figure 12: TM_{011}, 5-cells with wg and beam-pipe loads.

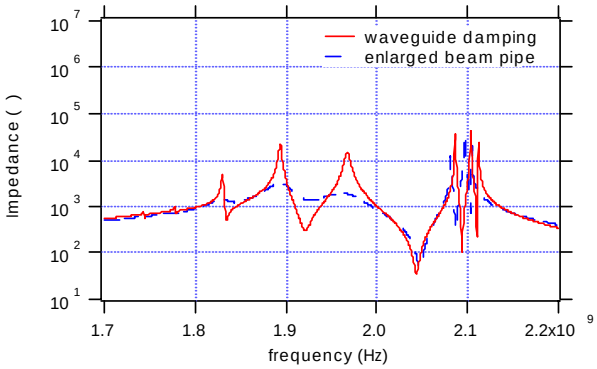

Figure 13: Dipole, 5-cells with wg and beam-pipe loads.

OTHER FACTORS

Other factors such as fabrication errors, distortion due to tuning, misalignment and loss of field flatness might contribute to higher than expected Q_{ext}'s. Field tilt in 7-cell CEBAF upgrade cavities has been observed to raise the Q_{ext} of some modes when the tilt is away from the end with the HOM couplers. Having dampers at both ends of the cavity guards against this. Having symmetrically arranged couplers so that no transverse kick is imparted to the passing beam is also desirable.

To go further in terms of broad-band HOM damping may require distributed HOM damping throughout the structure or perhaps damping apertures in each cell, e.g. fig. 14. This holds the promise of structures that may have constant damping properties independent of length and number of cells. Investigation of these types of structures is just beginning, and many technical questions have to be resolved before such structures might be usable.

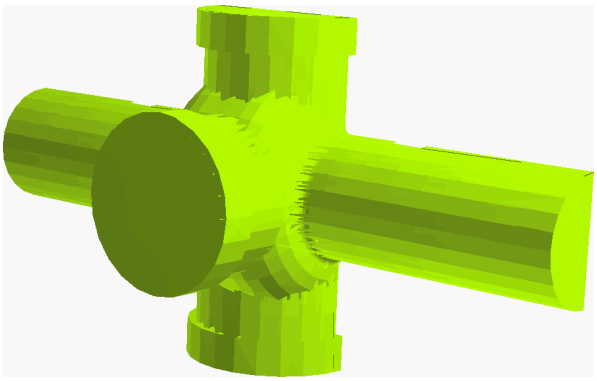

Figure 14: Cavity with damping apertures cut into the cell.

CONCLUSIONS

We have shown that strong broad-band HOM coupling techniques that are presently used on single-cell cavities can plausibly be applied to multi-cell cavities. None of the schemes described here can be considered optimized but all show promise. We have considered a variety of ways to couple the HOMs out of the cavity but ultimately the limit may be the rate at which energy can flow through the structure. To go significantly further we may want to look at more open structures, where energy is free to leave the system from any cell, or distributed damping along the structure between cells.

REFERENCES

[1] “Progress of the PEP-II B-Factory”, J. Seeman et. al, Proc. PAC03, Portland Oregon.

[2] “Present Status of the KEKB B-Factory”, H. Koiso et. al. Proc EPAC02, Paris, France.

[3] “Superconducting Cavities for HERA”, B. Dwersteg et.al., Proc. 3rd Workshop on RF Superconductivity, Argonne, IL, USA. ANL-PHY

[4] “Beam Impedance Calculation and Analysis of Higher Order Modes (HOMS) Damped RF Cavities Using MAFIA in Time Domain”, Derun Li , Robert A. Rimmer, Proc. PAC 2001, Chicago.

[5] “A Prototype Module of Superconducting Damped Cavity for KEKB” T. Furuya et. al., Proc. EPAC96, Barcelona, Spain.

[6] S. Belomestnykh et. al. "Commissioning of the Superconducting RF Cavities for the CESR Luminosity Upgrade", Proc. PAC99, New York.

[7] J.C. Amato, Proc. third Workshop on RF Superconductivity, Argonne, IL, USA. ANL-PHY-88-1, Vol.1., p 589, 1988.

[8] K. Hosoyama et al., “Crab Cavity for KEKB”, Proc. 7th Workshop on RF Superconductivity (1995).

[9] “Superstructures for High Current FEL Application”. J. Sekutowicz et.al., Proc. PAC03, Portland, OR.

[10]“Cavities for JLAB’s 12 GeV Upgrade”J. Sekutowicz et.al., Proc. PAC03, Portland, OR.